

Shape identification of unsteady heat convection fields to control temperature distribution

*†E. Katamine¹ and N. Okada²

¹Dep. Mechanical Engineering, National Institute of Technology, Gifu College, 2236-2 Kamimakuwa, Motosu-shi, Gifu, Japan

²Isuzu Engineering Co., Ltd. 8 Tsuchidana, Fujisawa-shi, Kanagawa, Japan

*Presenting author: katamine@gifu-nct.ac.jp

†Corresponding author: katamine@gifu-nct.ac.jp

Abstract

This paper presents numerical solution to a shape identification problem to control temperature distribution to a target distribution in sub-domains of unsteady heat convection fields. The square error integral between the actual temperature distributions and the target temperature distributions in the sub-domains during the specified period of time is used as the objective functional. Shape gradient of the shape identification problem is derived theoretically using the Lagrange multiplier method, adjoint variable method, and the formulae of the material derivative. Reshaping is carried out by the traction method proposed as an approach to solving shape optimization problems. Numerical analyses program for the shape identification is developed based on FreeFem++, and the validity of proposed method is confirmed by results of 2D numerical analyses.

Keywords: Inverse problem, Shape identification, Optimum design, Flow control, Traction method

Introduction

Shape design problems that improve the characteristics of heat transfer in thermal convection fields are an important subject in engineering. A typical example of such a problem can be seen in the design process used to create a heat exchanger. In this problem, the shape of the heat exchanger is optimized to maximize the heat discharge on the sub-boundaries of the convection field. Moreover, the problem of determining the boundary shape that can achieve the desired state distribution function of temperature or flow velocity on specified sub-boundaries, or in specified sub-domains, in a heat convection field is known as an inverse problem. If we regard the inverse problem as designing the shape needed to minimize the integrated squared error between the state distribution function of the actual temperature distribution and the target distribution function, then it can be treated as one optimization problem. This study discusses the solution of the inverse problem and the shape optimization problem with regard to the shape design of the heat convection field domain.

The theory of shape optimization for incompressible viscous flow fields was initiated by Pironneau [Pironneau(1973; 1974; 1984)], who formulated a shape optimization problem for an isolated body located in a uniform viscous flow field to minimize the drag power on this body. The distributed shape sensitivity, which is called the shape gradient, was derived with respect to the domain variation by means of an adjoint variable method based on optimal control theory. The adjoint variable method introduces adjoint variables into variational forms of the governing equations as variational variables; it also determines the adjoint variables using adjoint equations derived from criteria defining an optimality condition with respect to the domain variation.

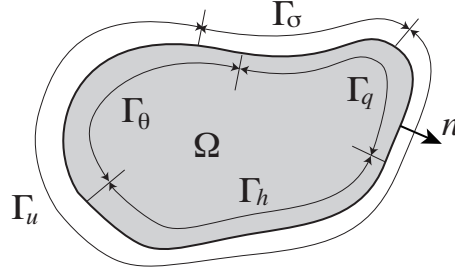


Figure 1: Heat convection field

The present authors have proposed an approach for the shape optimization of such channels or bodies based on a gradient method using the distributed shape sensitivity. In previous studies, the present authors presented a numerical method for the minimization of the dissipation energy of steady-state viscous flow fields [Katamine and Azegami(1995); Katamine et al.(2005)] and extended this method to 3D problems [Katamine et al.(2009)]. Also, the present authors applied this method to the shape optimization solution for the drag minimization and lift maximization of an isolated body located in a uniform viscous flow field [Katamine and Matsui(2012)] and the shape identification problem of flow velocity distribution prescribed problem in sub-domains of steady-state viscous flow fields [Katamine and Kanai(2016)].

The present study describes the extension of this method for solving a shape identification problem of unsteady forced heat convection fields to control temperature distribution to target distribution in sub-domains of the fields. Reshaping is accomplished using the traction method [Azegami et al.(1995; 1997); Azegami(2000)], which was proposed as a means of solving boundary shape optimization problems of domains. In the traction method, domain variations that minimize the objective functional are obtained as solutions of pseudo-linear elastic problems for continua defined in the design domain. These continua are loaded with pseudo-distributed traction in proportion to the shape gradient in the design domain.

In this study, the shape identification problem is formulated in the unsteady heat convection fields. The square error integral between the actual temperature distributions and the target temperature distributions in the sub-domains during the specified period of time is used as the objective functional. Shape gradient of the shape identification problem is derived theoretically using the Lagrange multiplier method, adjoint variable method, and the formulae of the material derivative. Reshaping is carried out by the traction method proposed as an approach to solving shape optimization problems. Numerical analyses program for the shape identification is developed based on FreeFem++, and the validity of proposed method is confirmed by results of 2D numerical analyses.

Governing equations for unsteady heat convection fields

Consider the unsteady heat convection field in the region Ω of \mathbb{R}^d ($d = 2, 3$) in time interval $[0, T]$. Consider determining the flow velocity $u(\vec{x}, t) = (u_i(\vec{x}, t))_{i=1,d}$, pressure $p(\vec{x}, t)$ and temperature $\theta(\vec{x}, t)$ at $\vec{x} \in \Omega$ and time $t \in [0, T]$. The dimensionless forms of the Navier–Stokes equation, continuity equation, and energy equation are the governing equations for unsteady heat convection fields. They can be expressed as follows:

$$\frac{\partial u_i}{\partial t} + u_j u_{i,j} = -p_{,i} + \frac{1}{Re} u_{i,jj}, \quad (\vec{x}, t) \in \Omega \times [0, T], \quad (1)$$

$$u_{i,i} = 0, \quad (\vec{x}, t) \in \Omega \times [0, T], \quad (2)$$

$$\frac{\partial \theta}{\partial t} + u_j \theta_{,j} = \frac{1}{RePr} \theta_{,jj}, \quad (\vec{x}, t) \in \Omega \times [0, T], \quad (3)$$

where the boundary $\Gamma = \partial\Omega = \Gamma_u \cup \Gamma_\sigma = \Gamma_\theta \cup \Gamma_q \cup \Gamma_h$, are Figure 1. Tensors described in this study use the Einstein summation convention and differentiation $(\cdot)_{,i} = \partial(\cdot)/\partial x_i$. The boundary conditions and initial conditions are described below:

$$u_i(\vec{x}, t) = \hat{u}_i(\vec{x}, t), \quad t \in [0, T], \quad \vec{x} \in \Gamma_u, \quad (4)$$

$$\sigma_i(\vec{x}, t) = \hat{\sigma}_i(\vec{x}, t) = (-p\delta_{ij} + \frac{1}{Re}u_{i,j})n_j = 0, \quad t \in [0, T], \quad \vec{x} \in \Gamma_\sigma \quad (5)$$

$$\theta(\vec{x}, t) = \hat{\theta}(\vec{x}, t), \quad t \in [0, T], \quad \vec{x} \in \Gamma_\theta, \quad (6)$$

$$-\frac{1}{RePr}\theta(\vec{x}, t)_{,j}n_j = \hat{q}(\vec{x}, t), \quad t \in [0, T], \quad \vec{x} \in \Gamma_q, \quad (7)$$

$$-\frac{1}{RePr}\theta(\vec{x}, t)_{,j}n_j = \hat{h}(\theta(\vec{x}, t) - \hat{\theta}_f), \quad t \in [0, T], \quad \vec{x} \in \Gamma_h, \quad (8)$$

$$u_i(\vec{x}, 0) = u_{i_{ini}}(\vec{x}), \quad \vec{x} \in \Omega, \quad (9)$$

$$p(\vec{x}, 0) = p_{ini}(\vec{x}), \quad \vec{x} \in \Omega, \quad (10)$$

$$\theta(\vec{x}, 0) = \theta_{ini}(\vec{x}), \quad \vec{x} \in \Omega. \quad (11)$$

Here, \hat{q} represents the heat flux, \hat{h} represents the coefficient of heat transfer, $\hat{\theta}_f$ represents the external temperature, δ_{ij} represents the Kronecker delta, Re is the Reynolds number, and Pr is Prandtl number. $(\hat{\cdot})$ represents the known function on the boundary. \vec{n} is an outward unit normal vector to the boundary. Also, $u_{i_{ini}}$ represents the initial flow velocity, p_{ini} represents the initial pressure, and θ_{ini} represents the initial temperature.

The weak forms of the respective governing equations (1)-(3) can be expressed with adjoint flow velocity $w(\vec{x}, t) = (w_i(\vec{x}, t))_{i=\overline{1,d}}$, adjoint pressure $q(\vec{x}, t)$, and adjoint temperature $\xi(\vec{x}, t)$ as follows:

$$\int_0^T \left\{ t^V(u_{,t}, w) + a^V(u, w) + b^V(u, u, w) + c(w, p) - l(w) \right\} dt = 0, \quad \forall w \in W, \quad (12)$$

$$\int_0^T \left\{ c(u, q) \right\} dt = 0, \quad \forall q \in Q, \quad (13)$$

$$\int_0^T \left\{ t^H(\theta_{,t}, \xi) + a^H(\theta, \xi) + b^H(u, \theta, \xi) + f_q^H(\xi) + f_h^H(\theta, \xi) - f_{hf}^H(\xi) \right\} dt = 0, \quad \forall \xi \in \Xi. \quad (14)$$

Furthermore, $t^V(u_{,t}, w)$, $t^H(\theta_{,t}, \xi)$, $a^V(u, w)$, $b^V(v, u, w)$, $c(w, p)$, $l(w)$, $a^H(\theta, \xi)$, $b^H(u, \theta, \xi)$, $f_q^H(\xi)$, $f_h^H(\theta, \xi)$, and $f_{hf}^H(\xi)$ are defined as follows:

$$\begin{aligned} t^V(u_{,t}, w) &= \int_\Omega w_i \frac{\partial u_i}{\partial t} dx, \quad t^H(\theta_{,t}, \xi) = \int_\Omega \xi \frac{\partial \theta}{\partial t} dx, \\ a^V(u, w) &= \int_\Omega \frac{1}{Re} w_{i,j} u_{i,j} dx, \quad b^V(v, u, w) = \int_\Omega w_i v_j u_{i,j} dx, \\ c(w, p) &= - \int_\Omega w_{i,i} p dx, \quad l(w) = \int_{\Gamma_\sigma} w_i \hat{\sigma}_i d\Gamma, \\ a^H(\theta, \xi) &= \int_\Omega \frac{1}{RePr} \xi_{,i} \theta_{,i} dx, \quad b^H(u, \theta, \xi) = \int_\Omega \xi u_j \theta_{,j} dx, \quad f_q^H(\xi) = \int_{\Gamma_q} \xi \hat{q} d\Gamma, \\ f_h^H(\theta, \xi) &= \int_{\Gamma_h} \hat{h} \xi \theta d\Gamma, \quad f_{hf}^H(\xi) = \int_{\Gamma_h} \hat{h} \xi \hat{\theta}_f d\Gamma. \end{aligned} \quad (15)$$

Here, $(\cdot)_t$ expresses the time derivative of the function. The flow velocity u , its adjoint w , and the other variables are considered to be elements of the following functional spaces:

$$U = \{u(\vec{x}, t) \in H^1(\Omega \times [0, T]) \mid u \text{ satisfies (4) and (9)}\}, \quad (16)$$

$$Q = \{q(\vec{x}, t) \in L^2(\Omega \times [0, T]) \mid \int_{\Omega} q \, dx = 0 \text{ (if } \text{measure}(\Gamma_{\sigma}) = 0)\}, \quad (17)$$

$$\Theta = \{\theta(\vec{x}, t) \in H^1(\Omega \times [0, T]) \mid \theta \text{ satisfies (6) and (11)}\}, \quad (18)$$

$$W = \{w_i(\vec{x}, t) \in H^1(\Omega \times [0, T]) \mid w_i(\vec{x}, t) = 0, \, t \in [0, T], \, \vec{x} \in \Gamma_u, \, w_i(\vec{x}, T) = 0, \, \vec{x} \in \Omega\}, \quad (19)$$

$$\Xi = \{\xi(\vec{x}, t) \in H^1(\Omega \times [0, T]) \mid \xi(\vec{x}, t) = 0, \, t \in [0, T], \, \vec{x} \in \Gamma_{\theta}, \, \xi(\vec{x}, T) = 0, \, \vec{x} \in \Omega\}. \quad (20)$$

Prescribing temperature in sub-domain in unsteady heat convection fields

In this section, the problem of minimizing the square integration errors between the actual temperature $\theta|_{\Omega_D \times [t_1, t_2]}$ from time $t = t_1 \in [0, T]$ to $t = t_2 \in [0, T]$ and the target temperature $\theta_D|_{\Omega_D \times [t_1, t_2]}$ in sub-domain $\Omega_D \subset \Omega$ is formulated. We assume $t_1 < t_2$. The domain transformation of this heat convection field region Ω is denoted by \vec{T}_s , and the domain Ω is assumed to vary to reach $\Omega_s = \vec{T}_s(\Omega)$ [Azegami et al. (1995; 1997)]. For simplicity, we assume that the sub-domains Ω_D and Γ_{σ} are invariable, that is $\vec{T}_s(\Omega_D) = \Omega_D$ and $\vec{T}_s(\Gamma_{\sigma}) = \Gamma_{\sigma}$ or domain variation. The square integration error problem for temperature distribution from time $t = t_1$ to $t = t_2$ is formulated as follows:

$$\begin{aligned} \text{Given } \Omega \quad \text{find } \Omega_s \quad \text{that minimizes } & \int_{t_1}^{t_2} E_{\Omega_D}(\theta) \, dt \quad \text{subject to (12) – (14) and} \\ & \int_{\Omega} dx \leq \beta_V M. \end{aligned} \quad (21)$$

where β_V is a coefficient related to the initial domain measure M , and

$$E_{\Omega_D}(\theta) = \int_{\Omega_D} (\theta - \theta_D)^2 \, dx. \quad (22)$$

The Lagrange function $L(u_i, p, \theta, w_i, q, \xi, \Lambda)$ for this problem is given as follows:

$$\begin{aligned} L = & \int_{t_1}^{t_2} E_{\Omega_D}(\theta) \, dt \\ & - \int_0^T \left\{ t^V(u_{,t}, w) + a^V(u, w) + b^V(u, u, w) + c(w, p) - l(w) \right\} dt - \int_0^T \left\{ c(u, q) \right\} dt \\ & - \int_0^T \left\{ t^H(\theta_{,t}, \xi) + a^H(\theta, \xi) + b^H(u, \theta, \xi) + f_q^H(\xi) + f_h^H(\theta, \xi) - f_{hf}^H(\xi) \right\} dt \\ & + \Lambda \left(\int_{\Omega} dx - \beta_V M \right). \end{aligned} \quad (23)$$

where $w \in W$, $q \in Q$, and $\xi \in \Xi$ were introduced as Lagrange multiplier functions or the adjoint functions with respect to the weak forms. The non-negative real constant number Λ is the Lagrange multiplier with respect to the volume constraint. The derivative of L with respect

to domain variation is derived using the velocity field $\vec{V}(\Omega_s) = \partial \vec{T}_s(\Omega) / \partial s = \partial \vec{T}_s / \partial s(\vec{T}_s^{-1}(\Omega_s))$, as follows [Azegami et al.(1995; 1997)]:

$$\begin{aligned}
\dot{L} = & - \int_0^T \left\{ t^V(u_{,t}, w') + a^V(u, w') + b^V(u, u, w') + c(w', p) - l(w') + c(u, q') \right\} dt \\
& - \int_0^T \left\{ t^H(\theta_{,t}, \xi') + a^H(\theta, \xi') + b^H(u, \theta, \xi') + f_q^H(\xi') + f_h^H(\theta, \xi') - f_{hf}^H(\xi') \right\} dt \\
& - \int_0^T \left\{ t^V(u'_{,t}, w) + a^V(u', w) + b^V(u', u, w) + b^V(u, u', w) + c(u', q) + b^H(u', \theta, \xi) + c(w, p') \right\} dt \\
& - \int_0^T \left\{ t^H(\theta'_{,t}, \xi) + a^H(\theta', \xi) + b^H(u, \theta', \xi) + f_h^H(\theta', \xi) \right\} dt + \int_{t_1}^{t_2} E_{\Omega_D}(\theta') dt \\
& + \dot{\Lambda} \left(\int_{\Omega} dx - \beta_V M \right) + l_G(\vec{V}).
\end{aligned} \tag{24}$$

Here, $(\cdot)'$ represents the derivative with respect to domain variation of the function fixed on the spatial coordinates, and

$$l_G(\vec{V}) = \int_{\Gamma} G \vec{n} \cdot \vec{V} d\Gamma, \tag{25}$$

and assuming that the flow velocity satisfies $u_i = 0$ at the design boundary,

$$\begin{aligned}
G &= G_0 + G_1 \Lambda, \\
G_0 &= \int_0^T \left\{ -\frac{1}{Re} w_{i,j} u_{i,j} - \frac{\partial \theta}{\partial t} \xi - \frac{1}{Re Pr} \xi_{,i} \theta_{,i} \right. \\
&\quad \left. - \nabla_n(\xi \hat{q}) - (\xi \hat{q}) \kappa - \nabla_n(\hat{h} \xi \theta) - (\hat{h} \xi \theta) \kappa + \nabla_n(\hat{h} \xi \hat{\theta}_f) + (\hat{h} \xi \hat{\theta}_f) \kappa \right\} dt \\
G_1 &= 1,
\end{aligned} \tag{26}$$

where $\nabla_n(\cdot) \equiv \nabla(\cdot) \cdot \vec{n}$, and κ denotes the quantity $(d-1)$ times the mean curvature of boundary, and $u_i, p, \theta, w_i, q, \xi$, and Λ are determined by the following conditions:

$$\begin{aligned}
& \int_0^T \left\{ t^V(u_{,t}, w') + a^V(u, w') + b^V(u, u, w') + c(w', p) - l(w') + c(u, q') \right\} dt = 0 \\
& \forall w' \in W, \forall q' \in Q
\end{aligned} \tag{27}$$

$$\int_0^T \left\{ t^H(\theta_{,t}, \xi') + a^H(\theta, \xi') + b^H(u, \theta, \xi') + f_q^H(\xi') + f_h^H(\theta, \xi') - f_{hf}^H(\xi') \right\} dt = 0 \quad \forall \xi' \in \Xi \tag{28}$$

$$\begin{aligned}
& \int_0^T \left\{ -t^V(u', w_{,t}) + a^V(u', w) + b^V(u', u, w) + b^V(u, u', w) + c(u', q) \right. \\
& \quad \left. + b^H(u', \theta, \xi) + c(w, p') \right\} dt = 0 \quad \forall u' \in U, \forall p' \in Q
\end{aligned} \tag{29}$$

$$\int_0^T \left\{ -t^H(\theta', \xi_{,t}) + a^H(\theta', \xi) + b^H(u, \theta', \xi) + f_h^H(\theta', \xi) \right\} dt - \int_{t_1}^{t_2} E_{\Omega_D}(\theta') dt = 0 \quad \forall \theta' \in \Theta \tag{30}$$

$$\Lambda \geq 0, \quad \int_{\Omega} dx \leq \beta_V M, \quad \Lambda \left(\int_{\Omega} dx - \beta_V M \right) = 0. \tag{31}$$

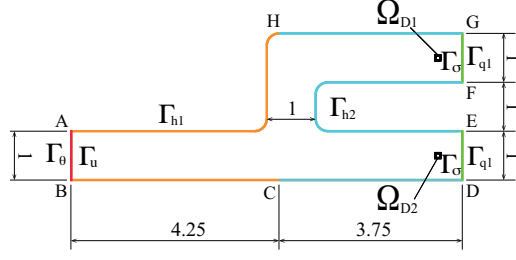


Figure 2: Numerical model: Branch channel, prescribing temperature distribution

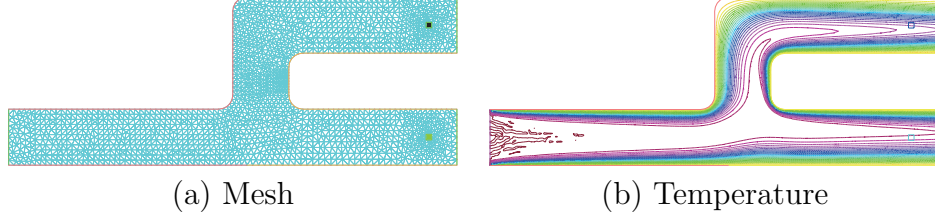


Figure 3: Numerical results: Mesh and temperature distribution at final time (t=400) for initial shape

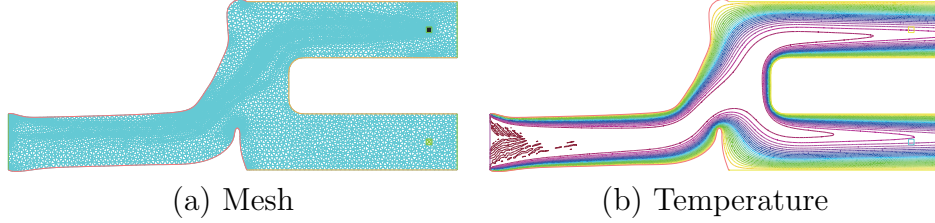


Figure 4: Numerical results: Mesh and temperature distribution at final time (t=400) for the identified shape

The derivative of the Lagrange function agrees with the derivative of the evaluation function, establishing the following relationship:

$$\dot{L}|_{u_i, p, \theta, w_i, q, \xi, \Lambda} = \dot{E}_{\Omega_D}|_{u_i, p, \theta, w_i, q, \xi, \Lambda} = l_G(\vec{V}). \quad (32)$$

Since $G\vec{n}$ in equation (25) is a coefficient function of the velocity field \vec{V} that provides minute variations in the domain, $G\vec{n}$ is referred to as a sensitivity function or shape gradient function. Furthermore, the scalar function G is referred to as the shape gradient density function.

Equation (27) is a weak form of the Navier–Stokes equation and the continuity equation (28) is a weak form of the energy equation in the state equation. Equation (29) is a weak form of the Navier–Stokes equation and continuous state equation for the adjoint problem, equation (30) is a weak form of the energy equation in the state equation for the adjoint problem, and (31) is a constraint equation related to the Lagrange multiplier Λ .

The traction method can be applied if the shape gradient function can be evaluated by analyzing $u_i, p, \theta, w_i, q, \xi$, and Λ based on these equations.

Numerical results

A shape identification problem for prescribing the temperature distribution $\theta|_{\Omega_D \times [t_1, t_2]}$ in an unsteady heat convection field was analyzed for the branch channel model shown in Fig.2.

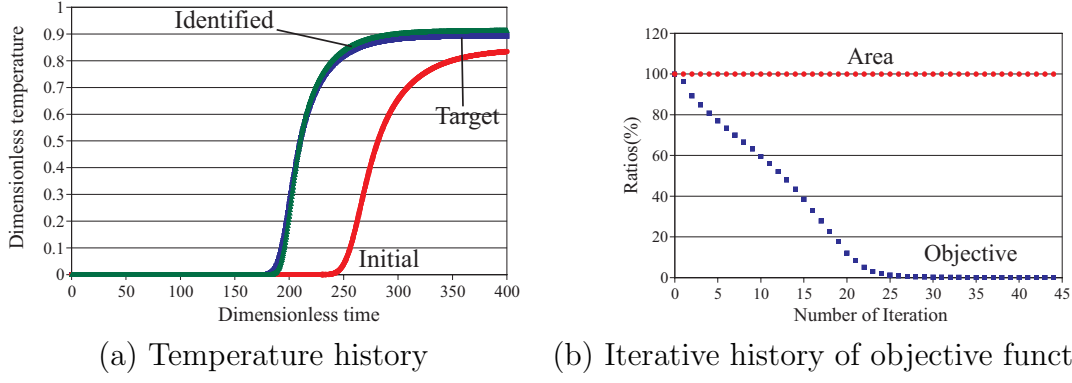


Figure 5: Numerical results: Temperature history in sub-domain Ω_{D1} and iterative history of objective functional

The hot thermal fluid flows in from a boundary Γ_u and flows out from two boundaries Γ_σ . The purpose of shape identification in this analysis is to unify the temperature distribution history near two outlet boundaries Γ_σ during the specified period of time. The temperature distribution history in sub-domain Ω_{D2} was set in the target distribution θ_D in Eq.(21), and the shape identification problem that the temperature distribution history in sub-domain Ω_{D1} agrees with the temperature distribution history in sub-domain Ω_{D2} was analyzed.

The flow boundary conditions included Poiseuille flow on an inlet boundary Γ_u and a natural boundary on two outlet boundaries Γ_σ . The temperature boundary conditions were as follows: $\hat{\theta} = 1$ on the inlet boundary Γ_θ , insulation boundary on the two outlet boundaries Γ_q , and the wall boundaries were heat transfer boundaries Γ_{h1} and Γ_{h2} , with a heat transfer coefficient $\hat{h} = 1$, and an external temperature $\hat{\theta}_f = 0$. The Reynolds number was $Re=100$ and the Prandtl number was $Pr=100$. The initial conditions of the entire domain were set to $\theta_{ini} = 0$ and $u_{i_{ini}} = 0$. The pressure was uniquely set to achieve an average of 0. The time was set to $t_1 = 0$ and $t_2 = T$, and time integration was performed from $t = 0$ to $t = T = 400$ with a $\Delta t = 0.4$ time increment. The two heat transfer boundaries Γ_{h1} of BC and HA were considered to be design boundaries Γ_{design} . Other boundaries were constrained with respect to domain variation. The coefficient β_V , which restrains the size of the domain, was set for $\beta_V = 1$. The heat transfer terms were not considered for the evaluation of the shape gradient density function in Eq.(26).

In this numerical analysis, the flow field velocity \vec{u} , pressure p , temperature θ , adjoint flow velocity \vec{w} , adjoint pressure q , adjoint temperature ξ , and shape updating analysis (velocity field \vec{V}) were all performed using FreeFem++[Ootsuka and Takaishi (2014)], [Hect (2012)]. The mesh and temperature θ at the end time $t = T = 400$ for the initial shape and the identified shape are shown in Fig.3 and Fig.4, respectively. Figure 5(a) shows the temperature history in the initial shape, a target temperature history, and the temperature history for the identified shape in sub-domain Ω_{D1} . Figure 5(b) shows the iterative history for the objective functional. Based on a comparison between Fig.3 and Fig.4, it was observed that the position of branch in the channel moved to upper part in the identified shape so that the temperature history of the two outlet boundaries agreed. In fact, it was confirmed that the temperature history in the sub-domain Ω_{D1} in the identification shape agreed with the target temperature history, and the objective functional approached zero from the result of Fig.5. According to this basic problem, the validity of the proposed method for the shape identification of the unsteady heat convection fields was confirmed.

Conclusions

In the present study, we formulated a shape identification problem in which the square error integral between the actual temperature distributions and the target temperature distributions on the prescribed sub-domains during the specified period of time on unsteady heat convection fields is used as the objective functional. The shape gradient of the shape identification problem was derived theoretically. The validity of the proposed method was confirmed based on the results of a 2D numerical analysis. The present study was supported in part by The OGAWA Science and Technology Foundation in Japan.

References

- [1] Pironneau, O.(1973) On Optimum Profiles in Stokes Flow, *J. Fluid Mechanics* **59**, Part 1, 117-128.
- [2] Pironneau, O.(1974) On Optimum Design in Fluid Mechanics, *J. Fluid Mechanics* **64**, Part 1, 97-110.
- [3] Pironneau, O.(1984) *Optimal Shape Design for Elliptic Systems*, Springer-Verlag.
- [4] Katamine, E. and Azegami, H.(1995) Domain Optimization Analyses of Flow Fields, *Computational Mechanics'95*, S. N. Atluri, G. Yagawa, and T. A. Cruse eds., Springer, **Vol. 1**, 229-234.
- [5] Katamine, E., Azegami, H., Tsubata, T., and Itoh, S.(2005) Solution to Shape Optimization Problems of Viscous Flow Fields, *International Journal of Computational Fluid Dynamics* **19**, 45-51.
- [6] Katamine, E., Nagatomo, Y., and Azegami, H.(2009) Shape optimization of 3D viscous flow fields, *Inverse Problems in Science and Engineering* **17**, No.1, 105-114.
- [7] Katamine, E. and Matsui Y.(2012) Multi-objective shape optimization for drag minimization and lift maximization in low Reynolds number flows, *Theoretical and Applied Mechanics Japan* **61**, 83-92.
- [8] Katamine, E. and Kanai R.(2016) Shape identification of steady-state viscous flow fields to prescribe flow velocity distribution, *Proceedings of the International Conference on Computational Methods*, Berkeley, CA, USA, G.R. Liu and Li, S. Eds, 41-45, ScienTech Publisher.
- [9] Azegami, H., Shimoda, M., Katamine, E., and Wu, Z. C.(1995) A Domain Optimization Technique for Elliptic Boundary Value Problems, *Computer Aided Optimum Design of Structures IV*, Hernandez S. and Brebbia C.A. eds., Computational Mechanics Publications, 51-58.
- [10] Azegami, H., Kaizu, S., Shimoda, M., and Katamine, E.(1997) Irregularity of Shape Optimization Problems and an Improvement Technique, *Computer Aided Optimum Design of Structures V*, Hernandez S. and Brebbia C. A. eds., Computational Mechanics Publications, 309-326.
- [11] Azegami, H.(2000) Solution to Boundary Shape Identification Problems in Elliptic Boundary Value Problems using Shape Derivatives, *Inverse Problems in Engineering Mechanics II*, Tanaka, M. and Dulikravich, G. S. eds., Elsevier, 277-284.
- [12] Ootsuka, K. and Takaishi ,T. (2014) *Finite element analysis using mathematical programming language FreeFem++*, Kyoritsu (in Japanese).
- [13] Hecht, F.(2012) New development in FreeFem++, *Journal of Numerical Mathematics*, **20**, 251-265.